MNRAS **000**, 1–15 (2015) Preprint 27 April 2016 Compiled using MNRAS LATEX style file v3.0

New orbit recalculations of comet C/1890 F1 Brooks and its dynamical evolution

Małgorzata Królikowska[1⋆] and Piotr A. Dybczyński[2], †
[1] *Space Research Centre of the Polish Academy of Sciences (CBK PAN), Bartycka 18A, 00-716 Warsaw, Poland*
[2] *Astronomical Observatory Institute, Faculty of Physics, A. Mickiewicz University, Słoneczna 36, 60-286 Poznań, Poland*

arXiv:1604.07538v1 [astro-ph.EP] 26 Apr 2016

Accepted XXX. Received YYY; in original form ZZZ

ABSTRACT

C/1890 F1 Brooks belongs to a group of nineteen comets used by Jan Oort to support his famous hypothesis on the existence of a spherical cloud containing hundreds of billions of comets with orbits of semimajor axes between 50 and 150 thousand au. Comet Brooks stands out from this group because of a long series of astrometric observations as well as nearly two-year long observational arc. Rich observational material makes this comet an ideal target for testing the rationality of an effort to recalculate astrometric positions on the basis of original (comet–star)-measurements using modern star catalogues. This paper presents the results of such new analysis based on two different methods: (i) automatic re-reduction based on cometary positions and the (comet–star)-measurements, and (ii) partially automatic re-reduction based on the contemporary data for originally used reference stars. We show that both methods offer a significant reduction of orbital elements uncertainties. Based on the most preferred orbital solution, the dynamical evolution of comet Brooks during three consecutive perihelion passages is discussed. We conclude that C/1890 F1 is a dynamically old comet that passed the Sun at a distance below 5 au during its previous perihelion passage. Furthermore, its next perihelion passage will be a little closer than during the 1890-1892 apparition. C/1890 F1 is interesting also because it suffered extremely small planetary perturbations when it travelled through the planetary zone. Therefore, in the next passage through perihelion it will be once again a comet from the Oort spike.

Key words: Solar system :general, Oort Cloud, comets:C/1890 F1 Brooks

1 INTRODUCTION

Jan Oort (1950) based his historic hypothesis on the existence of a distant, spherical cloud of cometary bodies surrounding the Solar system on the original $1/a$-distribution of nineteen near-parabolic comets with the best-determined (at that time) original orbits. Comet C/1890 F1 Brooks belonged to this group. It is distinguished by a long and rich series of observations: almost 2 yr period covered by about 900 positional measurements.

A question of the distribution of the reciprocal original semimajor axes $1/a_{\rm ori}$ is frequently repeated in the literature not only to support the Oort Cloud (OC) hypothesis, but also to examine the density distribution of the OC, recognized as a reservoir of the cometary bodies that can potentially penetrate into the planetary system (Fernández 2005). However, it was already established (Yabushita 1989; Dybczyński 2001; Królikowska & Dybczyński 2010; Dybczyński & Królikowska 2011), that a significant fraction of investigated comets with the original $1/a$ within the so-called Oort spike, $1/a_{\rm ori} \leqslant 10^{-4}\,{\rm au}^{-1}$, passed through the inner part of the Solar system in their previous perihelion passage. Therefore, the interpretation of the original $1/a$-distribution of the near-parabolic comets should be treated with caution. In particular, one should take into consideration that a vast majority of comets from the Oort spike suffered planetary perturbations that have changed significantly their semimajor axes during each deep passage through planetary zone. Here we focus our investigation on the dynamical history of Oort spike comets in the period extending back to their previous perihelion passage. It is the only direct method that allows us to separate the dynamically new comets of the Oort spike from the dynamically old ones.

Typical planetary perturbations defined by a change of $1/a$ during the passage within the inner part of the Solar system are typically two to four times greater than the present

⋆ E-mail: mkr@cbk.waw.pl
† E-mail: dybol@amu.edu.pl

© 2015 The Authors

estimate of the Oort spike width. In consequence, after visiting the inner planetary system, a comet has an excessive chance to be outside the Oort spike, leaving the Solar system on a hyperbolic orbit, or moving on a significantly tighter orbit than previously. Since many comets discovered so far will escape from the Solar system in the future, we also investigate their future evolution which gives a much broader perspective on the dynamical evolution of comets discovered as Oort spike comets (Dybczyński & Królikowska 2015, hereafter Paper 5 and references therein).

In addition to the above general arguments, there are also some specific objectives of the present investigation. We chose comet C/1890 F1 Brooks not only for its historic importance but also to develop and test our methods of data treatment for such a long-ago discovered comet. In the case of C/1890 F1, we have an opportunity to repeat the reduction of astrometric observations using contemporary star catalogues, typically much more precise, particularly in terms of proper motions. The ($\mathcal{C}-\star$)-measurements[1] ($\Delta\alpha$ in right ascension and $\Delta\delta$ in declination) are fortunately published in original papers together with calculated apparent comet positions for almost all observations of this comet. Apart from seven transit circle observations made in Washington the only sources without explicit ($\mathcal{C}-\star$)-differences are original papers reporting 99 observations from Bordeaux Observatory (only one paper with five observations from Bordeaux listed also ($\mathcal{C}-\star$)-measurements). Fortunately, these publications also consist of both, reference star identifications and their apparent places used for the reduction. Thereby, the reconstruction of the ($\mathcal{C}-\star$)-measurements is quite straightforward.

For all these reasons, we also decided to show in this paper how the determination of the observed osculating orbit[2]depends on the adopted method of data processing (how deep we are looking for sources of errors in the published data) and our choice of the catalogue for reference star positions. Two methods and two catalogues have been used for this purpose: PPM star catalogue (Roeser & Bastian 1988) and Tycho-2 star catalogue (Høg et al. 2000).

The first, fully automatic, method is very useful in cases in which we have at hand a list of astrometric cometary positions together with ($\mathcal{C}-\star$)-measurements in right-ascension and declination, and we had not entered data[3] on the reference stars originally used by observers. It involves the reconstruction of hypothetical star positions on the basis of ($\mathcal{C}-\star$)-measurements, and published cometary positions if they were given by observers. Otherwise, the cometary positions are estimated from preliminary orbital elements. Next, the re-reduction of these stars positions using PPM catalogue is carried out. Finally, the positions of comets are calculated based on obtained present-day star positions and original ($\mathcal{C}-\star$)-measurements. Of course, it can also be applied to a star catalogue other than PPM, but here the PPM catalogue is used for a comparison purpose. This method was successfully used for many comets discovered long ago (Gabryszewski 1997 and Królikowska et al. 2014), thus it is only very briefly described in section 3.1.

In this investigation however, all the data originally published by observers were collected. Therefore, a much more in-depth analysis of the original data can be done and the second method described in this paper is devoted to such an investigation. The Tycho-2 catalogue is chosen as it is perceived to be one of the best modern catalogues for this purpose, particularly regarding proper motions. In the first step, we collected a list of mean coordinates of all reference stars used by all observers and then their contemporary astrometric data were automatically obtained. Next, we calculated astrometric positions of the comet using ($\mathcal{C}-\star$)-measurements. Finally, manual and time consuming part was to investigate the causes of large residuals obtained from this automated step for about 30 per cent of all observations. About half of them resulted from the wrong star identifications and the rest came from some inconsistency or typographical errors in papers published by observers. More details about this second method are given in section 3.2.

The paper consists of seven sections. Next section describes the observational material and previous orbital determinations of C/1890 F1 Brooks that exist in literature. In section 3 details of the method of reference star position recalculation using the procedures based on PPM and Tycho-2 star catalogues are given, and a brief description of further steps of our data treatment is delivered.
A grid of osculating orbits based on both methods of reference star recalculations is described in Section 4, where also the analysis of differences between these results is presented. The original and future orbits are discussed in Section 5. The final result of this study, the most important from the dynamical point of view, is presented in Section 6, where we discuss what can be deduced about the origin of comet C/1890 F1 Brooks and its future dynamical evolution. The summary and conclusions resulting from this research are outlined in the last section.

2 OBSERVATIONS OF C/1890 F1 BROOKS AND STRÖMGREN'S ORBITAL DETERMINATION

Comet C/1890 F1 (called comet 1890a or 1890 II at that time) was discovered at Smith Observatory, Geneva, N.Y., USA by William R. Brooks on 1890 March 19, at 16 hours standard, 75th meridian time (March 20.38 UT, see Brooks (1890)) at a heliocentric distance of 2.1 au and 2.7 au from the Earth. The comet was extensively observed during next several months. In the first days of June 1890 the comet reached its perihelion at a distance of 1.91 au from the Sun (on June 2) and the day after – the closest distance of 1.57 au from the Earth.

The Cometography by Gary W. Kronk (2003, vol.2, pages 648-652) was very helpful in collecting rich literature concerning comet C/1890 F1 Brooks. It appeared that all these original papers are nowadays available in an electronic form what highly accelerated our data processing. Thanks

[1] (comet−star)-measurements
[2] that is always the starting nominal orbit for our numerical calculations of dynamical evolution
[3] Large sets of such data typed in computer files were prepared during a long campaign of collecting observations of one-apparition comets as a part of the Warsaw Catalogue of Cometary Orbits project (Królikowska et al. 2014).

Table 1. List of all observatories involved in observing comet C/1890 F1 Brooks. The last observatory (Shattuck Observatory operated by Dartmouth College in Hanover, New Hampshire) was not present in the standard MPC list of observatories at the time when we performed our calculations. Therefore, it had our new code marked by negative number: −58. Now, this observatory is included in the list and its code is 307. In our basic set of data we omitted: seven transit observations from Washington, four unpublished observations from Liège, and additional nine from Vienna as they were published after the monumental Strömgren's (1896) paper, see text for more details.

Observatory code & place	Number of measurements	Observatory code & place	Number of measurements
000 Greenwich	62	004 Toulouse	17
007 Paris	5	008 Algiers-Bouzaréah	13
014 Marseilles	25	020 Nice	18
035 Copenhagen	21	045 Vienna	78 + 9
084 Pulkovo	54	085 Kiev	58
089 Nikolaev	9	135 Kasan	33
513 Lyons	3	516 Hamburg	72
522 Strasbourg	8	526 Kiel	13
528 Göttingen	36	529 Christiania	27
531 Collegio Romano, Rome	12	532 Munich	26
533 Padua	15	537 Urania Obs., Berlin	13
539 KremsmÃijnster	38	548 Berlin	6
582 Orwell Park Obs., Ipswich	15	601 Dresden, Engelhardt Obs.	13
623 Liège	4	662 Lick Obs., Mount Hamilton	13
753 Washburn Obs., Madison	6	767 Ann Arbor	16
780 Leander Mc Cormick Obs., Charlottesville	8	787 U.S. Naval Obs., Washington	22 + 7
794 Vassar College Obs., Poughkeepsie	9	802 Harvard Obs., Cambridge	12
999 Bordeaux-Floirac	99	-58 Hanover, Shattuck Obs., New Hampshire	13

Table 2. Global description of all available astrometric observations of C/1890 F1 Brooks. Our basic set of collected data consists of 888 positional measurements that cover the same time-interval as given in the fourth column (see text for an explanation).

Comet name	q_{obs}	T	Observational arc dates	No of obs	Data arc span	Heliocentric distance span
	[au]	[yyyy mm dd.ddddd]	[yyyy mm dd − yyyy mm dd]		[yr]	[au]
C/1890 F1 Brooks	1.908	1890 06 02.03838	1890 03 22 − 1892 02 05	908	1.9	2.11 − 6.56

to the NASA's Astrophysics Data System Bibliographic Services (ADS) [4], we were able to gather full original versions of almost all sources listed by Kronk, except for the papers published in *Comptes Rendus*. The latter are available at the French *Gallica* digital library [5].

Additionally, an extensive study of C/1890 F1 Brooks published by Elis Strömgren (1896) was extremely helpful in our investigation. Unfortunately, this book is not available from the ADS, however it can be found at *Hathi Trust Digital Library* [6]. Strömgren collected all available [7] positions (899 in number) spanning the entire period of measurements. Then, in contemporary catalogues he identified almost all reference stars used by observers several years earlier, and on this basis he recalculated almost all comet's positions. The final osculating orbit obtained by him is based on 854 observations reduced again, carefully weighted and then grouped in sixteen normal places spread over the period from 1890 March 20 to 1892 February 05. Next, he added approximate perturbations by Earth, Mars, Jupiter, and Saturn. This solution is presented in many sources as the most credible osculating orbit for this comet. For example, an osculating orbit given in the last edition of the Catalogue of Cometary Orbits Marsden & Williams (2008, hereafter MWC08) is cited as an orbit derived by Strömgren, however the epoch of orbit is taken close to perihelion passage (1890 June 2), whereas Strömgren adopted the osculation epoch close to the beginning of data sequence (1890 March 17). It means that osculating orbit derived originally by Strömgren was dynamically evolved a two and a half months forward for the MWC08 purposes and finally transferred to the J2000 reference frame.

In Table 1, the list of all observatories involved in observing the comet C/1890 F1 according to Strömgren's paper is presented (36 observatories, page 31 therein). We independently collected 888 original cometary positions given by observers in their original papers and this set of data is used here as 'basic set of original cometary positions' (hereafter 'basic set of data') , which were next recalculated using the PPM star catalogue.

One can see that almost 50 per cent of all data were gathered in six of presented observatories: Bordeaux (99 measurements), Vienna (87), Hamburg (72), Greenwich (62), Kiev (58) and Pulkovo (54).

All the collected data are plotted in Fig. 1, where discovery position is given by magenta point, pre-perihelion data are shown as dark-turquoise points, and light-turquoise points follow the post-perihelion trajectory on the sky.

Global characteristics of the collected observational material are given in Table 2. The asymmetry in observed helio-

[4] http://adswww.harvard.edu/
[5] http://gallica.bnf.fr/
[6] https://www.hathitrust.org/
[7] After his investigation nine more measurements taken in Vienna were published and these are also included in our orbit determination using Tycho-2 star catalogue.

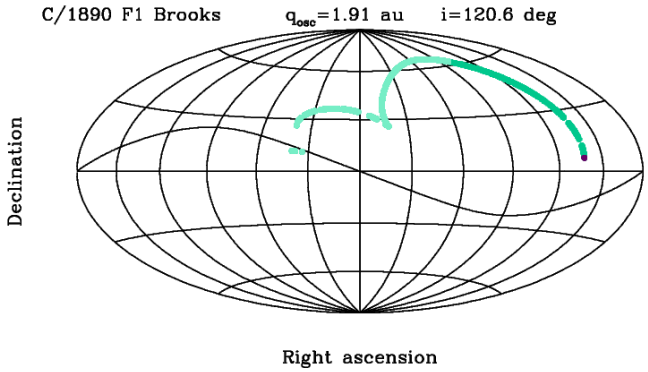

Figure 1. The overall view on cometary track of C/1890 F1 Brooks filled by collected astrometric observations in geocentric equatorial coordinate system given in Aitoff projection. Declination is plotted along the ordinate, right ascension is plotted along the abscissa (increasing from zero to 360 degree from the left to right) and the centre of projection is at 0°declination and 180°right ascension. The lines of right ascension and declination are shown at 30°intervals and the wavy line shows the projection of the ecliptic onto the celestial sphere. Each positional observation before perihelion passage is shown as a dark turquoise point, except the first observation that is shown by a dark magenta point whereas the data taken after perihelion passage are marked by light turquoise points.

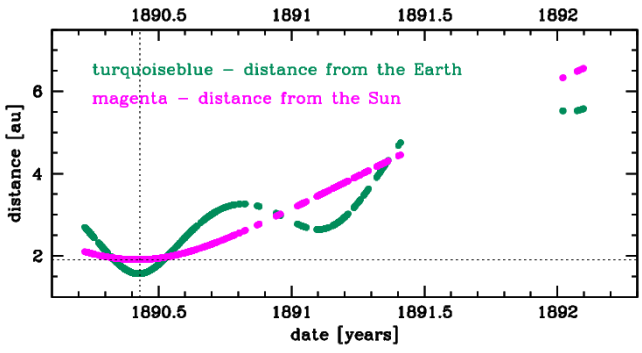

Figure 2. The time distribution of positional observations of C/1890 F1 Brooks with corresponding heliocentric (magenta curve) and geocentric (turquoise curve) distance at which they were made. Horizontal dotted line shows the perihelion distance and vertical dotted line the moment of perihelion passage.

centric distances around perihelion is easily visible in Fig. 2 (magenta track), where one can see that C/1890 F1 was discovered at a distance of about 2.1 au from the Sun and was followed far after the perihelion passage (1.9 au) to about 6.7 au from the Sun. In the entire dataset of C/1890 F1, there are only two photographic measurements, taken by Charles Trépied on 1890 May 22 at Algiers Observatory. It is also worth noting here that Stéphane Javelle (Nice Observatory) was the only observer who followed the comet after the seven-month gap in the data due to comet's conjunction with the Sun.

3 TWO METHODS OF DATA PROCESSING

In our orbit recalculation presented here, we primarily relied on original data published by observers. We also partially based our analysis on the Strömgren's (1896) paper where the whole set of data is published. However, we only used ($\mathcal{O}$−$\star$)-type of Bordeaux observations given there, and, optionally, corrections to all 99 cometary positions in declination taken in Bordeaux since both types of data were not published anywhere else. The author received them directly from Georges Rayet, the director of Bordeaux observatory. Therefore, to be as close to Strömgren's sample of observations as possible, our 'basic set of data' consists of 888 positional observations, all with given ($\mathcal{O}$−$\star$)-type of measurements. Our full sample of data includes twenty more observations (from Washington, Vienna and Liège Observatories, see Tables 1 and 2).

The only intervention into the original data are our manual corrections of typing mistakes which sometimes appear in published tabular data, or explicit observer's errors manifesting as a kind of outliers (e.g. distant from preliminary orbit by full number of minutes in right ascension or/and declination). Some of them were identified by Strömgren, often by a direct contact with observers. Thus, we took almost all of them into account and we also identified several more. The complete list of the adopted corrections can be found at our `WikiComet` page [8] in the supplementary material to this paper.

Next, we used direct measurements of comet positions relative to reference stars, that is the ($\mathcal{O}$−$\star$)-type of data, in order to recalculate new positions of the comet using more modern star catalogues. For this purpose, we used two different approaches based on PPM and Tycho-2 catalogues, respectively.

3.1 Method I of comet position recalculations

The first method used here is based on the reverse process to the one performed by observers. The star position is calculated from the ($\mathcal{O}$−$\star$)-measurements listed by an observer and from a given cometary position and next corrected using the PPM star catalogue (Gabryszewski 1997). Sometimes in original papers only ($\mathcal{O}$−$\star$)-measurements are given (in right ascension and/or in declination). When comet's position is not given in one or both of the coordinates, we temporarily calculate the values of the missing coordinates which fit the cometary orbit, and then we are looking for a matching star. If successful, we obtain a position of the comet in the previously unknown one or two coordinates. This method does not require any identification of individual reference star and its mean position, because if we can find (in the PPM star catalogue in this realisation) a star within a radius of few tens of arc seconds from the original position adopted by an observer, then we are sure in practice, that this is the correct star. More details about this procedure applied for recalculating comet positions are described by Gabryszewski (1997) and next by

[8] `http://apollo.astro.amu.edu.pl/WCP`

Table 3. The process of preliminary determination of the osculating orbit: comparison between original data and data recalculated using PPM star catalogue. For Bordeaux set of data (subset B, both version) selection in steps 1a and 1b was limited to the rejection of three largest outliers. In the remaining cases a sharp Bessel criterion was applied for data selection during the process of orbit determination; the resulting cut-off level (all measurements that give larger residuals are not taken into account) is displayed in columns [3]/[6] and [9].

Data description	Number of measurements	Before PPM Step I			After PPM Step II using the same limit for outliers			After PPM Step III repeated selection procedure		
		Level of cut-off	Number of residuals	rms	Level of cut-off	Number of residuals	rms	Level of cut-off	Number of residuals	rms
[1]	[2]	[3]	[4]	[5]	[6]	[7]	[8]	[9]	[10]	[11]
subset A	789	17.″0	1380	5.″08	17.″0	1421	4.″71	14.″7	1404	4.″35
subset B, version O	99	25.″0	197	6.″95	25.″0	198	6.″11	15.″1	193	5.″41
subset B, version C	99	25.″0	197	5.″51	25.″0	198	4.″46	8.″9	193	3.″20

Królikowska et al. (2014) who presents the successful application of this approach to 38 Oort spike comets discovered in the first half of the twentieth century.

When a certain fraction of the reference stars is successfully found for a given sample of observations, this procedure always leads to an improvement of the orbit determination by (i) reduction of the root mean square (rms) residual and/or by (ii) enlargement of the number of applicable observations for orbit determination. Thus, it also leads to smaller uncertainties of orbital elements. Therefore, we often use this method as an effective tool for extensive studies based on large samples of comets. For this method we decided to take a sample of 888 observations with known ($\mathscr{O}-\star$)-measurements, including the set of 99 measurements from Bordeaux. There are 38 observations where only ($\mathscr{O}-\star$)-type of data are given in original papers, and a few dozens more for which the difference in ($\mathscr{O}-\star$), and as a consequence the cometary position, is given in only one coordinate (in right ascension or in declination). Since Strömgren recalculated comet's positions for almost all measurements using more modern catalogues than were previously available to the observers, it will be interesting to compare here his osculating orbit of C/1890 F1 with our orbital results based on automatic search for reference stars in the PPM catalogue, and next with the results obtained with a different re-reduction algorithm and Tycho-2 catalogue (Section 3.2).

As we mentioned before, Strömgren published the corrections to declinations for Bordeaux measurements, which he received directly from Rayet who observed C/1890 F1 five years earlier. Since the literal application of all these corrections does not seem to be obvious (see Section 3.2 for an in-depth discussion on these corrections), we divided the data into two subsets: one containing only Bordeaux measurements (subset 'B') and the other with all remaining observations from the basic set of 888 measurements (subset 'A'). Next, we applied the PPM procedure to both, independently; and additionally we performed this step for two variants of subset 'B' data. In version 'O', we dealt with the original measurements, whereas in version 'C' the corrections to $\Delta\delta$ published in pages 32–33 of Strömgren's paper were applied. The PPM procedure gave the same results for 'O' and 'C', what was expected. Namely, using the PPM procedure, corrected positions for the same 51 reference stars of 99 original measurements were found. In the case of subset A containing 789 observations, the reference star positions for 402 measurements were recalculated. Next, for each of three subsets of data (each containing about 50 per cent of recalculated cometary positions), the same sharp Bessel selection criterion was independently applied during the process of osculating orbit determinations (for more details about our methods of data selection see Królikowska et al. (2009), and references therein). The results are summarized in Table 3 and the main conclusions from these steps of data processing are as follows:

- Automatic search procedure for reference stars in PPM (Gabryszewski 1997) allowed us to find new star positions for about 50 per cent of measurements in the case of C/1890 F1, while Strömgren found manually about 92 per cent of stars in catalogues available to him in 1896. The difference in the effectiveness of star search results not only from the manual approach applied by Strömgren, but also from the fact that the method discussed now, ignores, for purposes of comparison, the data on the stars used by the observers and Strömgren. These original stellar data are used in our second method (see section 3.2).
- This recalculation of star positions significantly improved the rms of the whole data sets – compare columns [5] and [11] of Table 3. The most spectacular decrease of rms was obtained for Bordeaux data when the Rayet corrections were applied to $\Delta\delta$ measurements and, as a consequence, to original comet positions in δ for these measurements.
- Rayet corrections to positions in declination appeared to significantly improve the rms at each step of orbit determination (compare columns [5], [8] and [11] in the variant C and variant O)

Since Rayet corrections to declinations significantly reduced scattering of data points around the orbit determined from Bordeaux measurements (these data are spread over a relatively long arc of orbit corresponding to the time interval of about 1.1 yr), we decided to construct two types of data recalculated using the PPM star catalogue:

- DATA_Ia where Rayet corrections were ignored,
- DATA_Ib where Rayet corrections were applied,

to show how the orbit changed under the influence of these $\Delta\delta$-corrections suggested by Rayet for Bordeaux measurements, which represent about 11 per cent of the whole set of data and only in declination.

At the end of this section it is interesting to trace the relative weights of those observatories, where the largest number of data were taken. We decided to weigh the measurements according to the place where they were made and whether they are successfully converted using the PPM catalogue or not. Therefore, Table 4 (columns [1]–[5]) gives rela-

tive weights for subsets of original measurements, that is for those where stars were not found in PPM catalogue (column [4]), and for subsets where stars were found and cometary positions were recalculated (column [5]). We found that for all these subsets of measurements the recalculated parts are less dispersed around the cometary orbit than those consisting of original positions. This fact is manifested in higher weights in column [5] than in column [4] for each observatory given in Table 4. A spectacular improvement of comet's position residuals is found for Pulkovo Observatory (Russia). In fact, astrometric measurements taken by Franz Renz using the 38-centimetre (15-inch) refracting telescope are the best in the whole data set for C/1890 F1.

Summarizing, Tables 3–4 show that the use of automatic search for star position in modern star catalogue (here: PPM catalogue); starting only with comet's positions and ($\mathscr{C}-\star$)-measurements in hand significantly improves positional observations of comets discovered long ago.

3.2 Method II. In-depth method of comet position recalculation using Tycho-2 catalogue

The second, partly automatic and therefore more time consuming method of positional measurements handling was initially inspired by the monumental work of Elis Strömgren (1896), which has been already mentioned in previous sections. The main idea is generally the same: use only the ($\mathscr{C}-\star$)-measurement, take mean coordinates of the reference star used by the observer and calculate a comet position using this star position taken from the most precise source. Strömgren collected 899 observations of C/1890 F1 Brooks and completed a list of 486 different reference stars used by observers. It seems worth to mention that for 17 stars Strömgren himself calculated proper motions which were unavailable at that time. On the other hand, he rejected 40 stars as having no reliable catalogue positions available to him and, as a result, he discarded 45 observations based on these stars. In his paper he noted that additional five observations were published after his work was completed, and in fact we found nine such additional observations, all from Vienna observatory. We found all the original papers containing C/1890 F1 observations, except for four observations made by dr De Baal at Liège Observatory, which Strömgren obtained in a private communication and which probably were never published separately. In the case of these four observations we used data given in Strömgren's paper.

Since our aim here was to recalculate cometary positions using ($\mathscr{C}-\star$)-type of measurements and contemporary stellar data, we excluded seven meridian circle observations made at Washington (Superintendent of USNO 1890) from this procedure. We only reconstructed the moments of these observations taken from this original communication. Additionally, a problem with Bordeaux observations also appeared: among 99 measurements only in five cases the published data contained differences ($\mathscr{C}-\star$). We decided to use the differences presented by Strömgren (1896), which he reconstructed from original publications or obtained (along with the above mentioned corrections) in the course of personal communication with Georges Rayet, the Bordeaux Observatory director at that time.

Our first step was to supply a list of mean stellar positions copied from Strömgren's list of reference stars, as a search target for the SIMBAD database [9]. Strömgren's stellar data were so good that 88 per cent of stars were automatically found within the radius of 10 arcsec. Another 11 per cent (50 of 446 stars) was found in the distance between 10 and 30 arcsec, and only a few stars in distances larger than 30 arcsec from the positions given by Strömgren. However, there were numerous ambiguous identifications, and of course not all of the indubitable identifications were correct, so a lot of manual search and corrections was necessary. Next, we tried to identify those 40 stars for which Strömgren presented no coordinates, and all of them were found in SIMBAD database by using information given by observers in their original papers. We also found seven additional stars used for nine Vienna observations unavailable for Strömgren because these measurements were published after his paper was. In all, we obtained a list of 491 SIMBAD identifications of the reference stars used by C/1890 F1 observers (surprisingly, there are two stars from Strömgren's list that were not used by any observer). We were interested in the most precise astrometric parameters of these stars. About 40 per cent of them could be found in the Hipparcos Catalogue (Perryman et al. 1997) but due to the importance of proper motions and the necessity to use internally consistent data, we decided to use Tycho-2 catalogue as a source of positions and proper motions. We found Tycho-2 identifications for all of 491 reference stars, and only for five of these stars there are no solution given in this catalogue (these stars are marked with the 'X' flag - "no mean position, no proper motion"), so we decided to use positions and proper motions from the UCAC4 catalogue (Zacharias et al. 2013) for them. This addition to Tycho stars is so small that in the remaining text we call the stellar data source simply the Tycho-2 catalogue.

In order to avoid unnecessary calculations for individual observations, we have introduced the following algorithm.

- First, we corrected a reference star position for its proper motion from the standard epoch of J2000 to the moment of observation. These corrections were to be considered for the relatively large time-interval of 110 years and we used also parallaxes and radial velocities from SIMBAD database whenever they were available.
- Second, we applied an appropriate precession matrix to express star coordinates in a mean reference frame of the epoch of observation.
- Next, we added the measured ($\mathscr{C}-\star$) differences.
- At the end, we reversed the precession calculation from the second step above.

As a result a list of 901 astrometric, topocentric positions of a comet was obtained. Moreover, they were expressed in the J2000 ICRS frame and ready for orbit determination. Such a procedure allows us to omit, for example, corrections for nutation, aberration etc. At the end we added seven meridian observations from Washington (with the epochs of observations reconstructed from local sidereal times), making the total number of observations in DATA_II set equal to 908. Among them 84 observations consisted of only one coordi-

[9] http://simbad.u-strasbg.fr/simbad/

Table 4. Relative weights for six observatories with the largest number of measurements for three versions of data handling: DATA_Ib (columns [4] & [5]), DATA_IIa (column [6]) and DATA_IIb (column [7]).

Observatory location	Number of all obs.	Per cent of obs. recalculated using PPM catalogue	Relative weights: Data_Ib – weighted solution: original part of obs. (star in PPM not found)	Data_Ib – weighted solution: part of obs. recalculated using PPM	Data_II – weighted solution: recalculated using Tycho-2 catalogue, corr. for Bordeaux omitted	Data_II – weighted solution: recalculated using Tycho-2 catalogue, corr. for Bordeaux included
[1]	[2]	[3]	[4]	[5]	[6]	[7]
Bordeaux	99	50.5	0.738	0.795	0.529	1.232
Vienna	78	62.8	0.515	0.604	0.630	0.623
Hamburg	72	54.2	0.869	1.031	1.121	0.821
Greenwich	62	48.4	0.422	0.515	0.372	0.318
Kiev	58	46.6	0.609	0.619	0.683	0.561
Pulkovo	54	66.7	1.458	3.406	3.874	3.602

Figure 3. O-C diagrams for comet C/1890 F1 Brooks with DATA_IIb-version of observations. Two upper panels present the time distribution of positional observations with corresponding residuals based on unweighted data (orbital solution A1) and weighted data (orbital solution A5), respectively, where residuals in right ascension are shown as green dots and in declination as red triangles. The lowest panel shows relative weights for solution A5. Note that the horizontal axes show the time elapsed from the beginning of the 1890 AD.

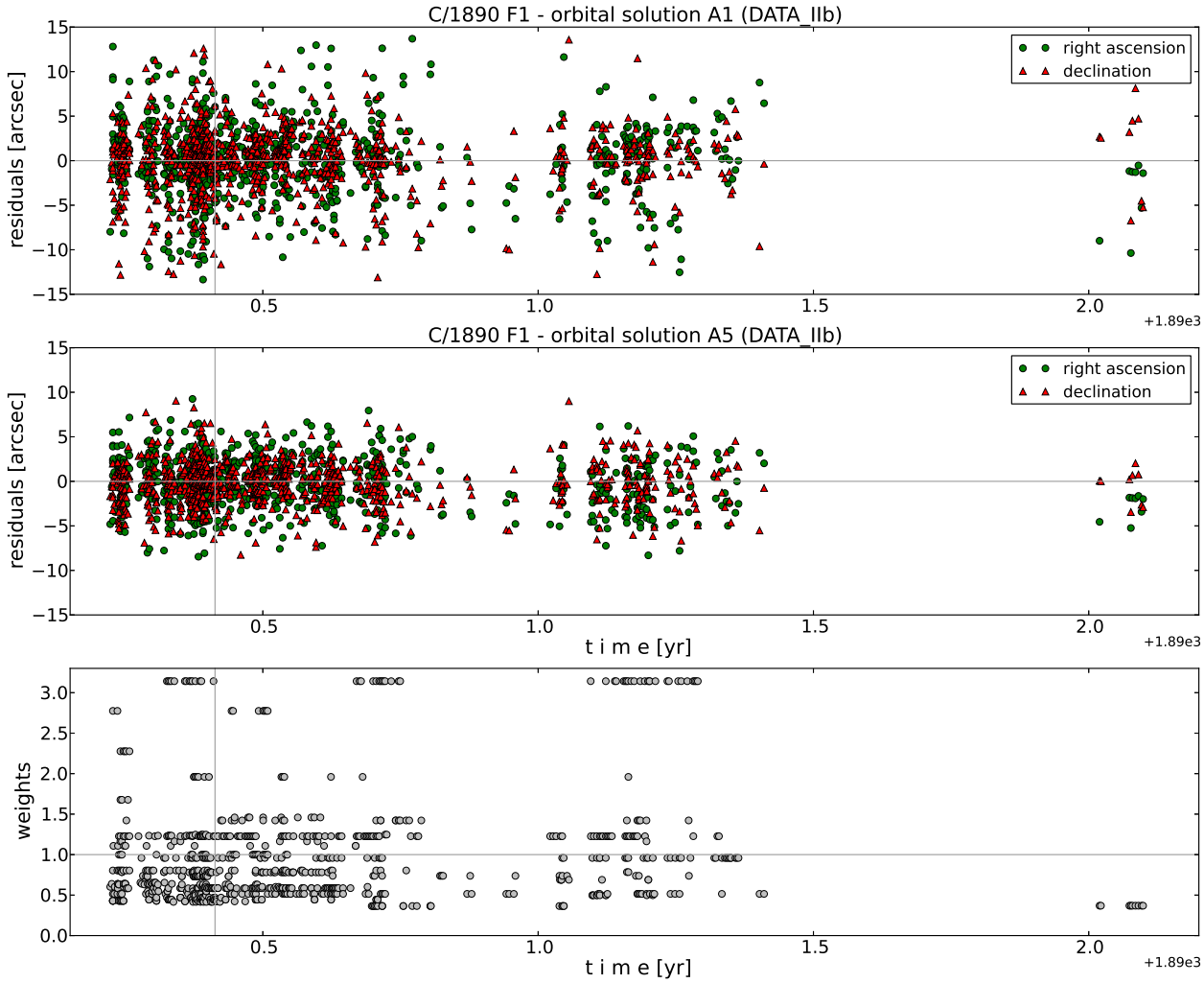

nate (right ascension or declination) what made a number of 1732 residuals potentially suitable for orbit determination.

Preliminary calculation of the O-C residuals with respect to the Strömgren's orbit revealed numerous large residuals. Deep inspection of each case allowed us to eliminate most of the suspected gross errors. In this process, we confirmed most of the corrections proposed by Strömgren (see notes at pages 70–71 of his paper), sometimes finding different explanations. We also introduced a certain number of new corrections, eliminating some incorrect reference star identifications or various typos found in original papers.

Special attention was given to the corrections of north polar distance (NPD) for all Bordeaux observations, published by Strömgren after he had received them from Rayet through personal correspondence. Strömgren quoted the Rayet explanation for these corrections: "Les observations de la Comète 1890 II ont été, à l'origine, réduites avec une valeur inexacte du tour de la vis de déclinaison de l'éqvatorial". All these corrections were carefully checked and it appeared that they can be divided into two groups: most of them are linear functions of the observed NPD differences (as expected) but about 10 per cent seems to be somehow modified. To discriminate between these two groups we performed least square fitting that allowed us to obtain a simple formula for **linear** corrections:

$$NPD_{\rm cor} = 0.016981 \times \Delta NPD + 0.010516, \qquad (1)$$

where ΔNPD is a published difference in NPD measured by an observer and $NPD_{\rm cor}$ is the calculated correction and both are expressed in arc seconds. After a detailed inspection we decided to apply all corrections that are linear with respect to the observed NPD as fully legitimate and eight individual, additional corrections proposed by Strömgren or found by us as probable typing errors in original papers. The list of all corrections applied by us (not only for the Bordeaux observations) can be found in an auxiliary material to this paper, see the note at the end of this paper.

Similarly as in section 3.1, we constructed here two versions of data (with and without corrections to Bordeaux ($\mathcal{C}-\star$)-measurements) recalculated with the use of Tycho-2 catalogue to study their overall influence on the resulting comet orbit:

- DATA_IIa where corrections to $\Delta\delta$ of Bordeaux measurements were ignored,
- DATA_IIb where corrections to $\Delta\delta$ of Bordeaux measurements were applied.

However, in the DATA_IIb set we decided to apply corrections for Bordeaux declinations calculated from the linear model (described above) instead of those listed by Strömgren and based on Rayet's estimations.

Columns 6 and 7 of Table 4 show that the Bordeaux subset of data is about 2.5 times less scattered along the orbit when these corrections for $\Delta\delta$ are applied. As a result Bordeaux subset of data in the DATA_IIb (column 7) has greater weights than subsets of data from Vienna, Hamburg, Greenwich and Kiev, while without these corrections the situation is reversed.

4 NEW OSCULATING ORBIT DETERMINATIONS

In the previous section, we constructed two versions of data for each of two methods of data recalculations. We are convinced that the most reliable osculating orbit is based on data recalculated with the use of the Tycho-2 star catalogue, including the corrected Bordeaux $\Delta\delta$-measurements according to linear formula given by Eq. 1, and involving the deep data processing to eliminate as many sources of errors as possible (a solution based on DATA_IIb).

However, to put the problem of orbit determination into a wider perspective, we constructed here a grid of osculating orbit starting from 2×2 sets described in Section 3. Then, for each of them we performed two types of final data treatment during the process of orbit determination:

- selection procedure based on Bessel criterion (hereafter called A1 type of solution),
- selection and weighting procedure (hereafter called A5 type of solution); for our methods of data weighting see Królikowska et al. (2009) or Królikowska & Dybczyński (2010).

It should be emphasized that the process of data selection (and weighting) is individually performed for each data set and each type of model of motion (ballistic or non-gravitational), separately. In other words, it is always carried out simultaneously during the iterative process of osculating orbit determination. In this paper we present only purely gravitational solutions (ballistic) because non-gravitational effects are very poorly determinable (pre-perihelion branch of orbit covered by data is distributed only over a two-months period and perihelion distance reaches 1.9 au, see also a very narrow range of the observed heliocentric distances before perihelion in Fig. 2). Thus, we decided to not include such uncertain solutions in the presented here analysis.

The grid of final osculating orbits is presented in Table 5 and the O-C-diagram for DATA_IIb-version of observations is shown in Fig. 3. In Table 5 we omitted only two unweighted solutions for data sets constructed without the Bordeaux corrections. Nevertheless, these solutions are shown in Fig. 3 with magenta symbols. All osculating orbits given in Table 5 are of the 1A quality class using Marsden et al. (1978) quality class assessment. However according to a modified method that we have recently introduced (Królikowska & Dybczyński 2013), we noticed differences in quality classes: solutions based on unweighted data are of 1b class, whereas solutions based on weighted observations are of 1a class (see column [1] of the table). We consider the orbit based on the weighted data which was previously recalculated with the use of the Tycho-2 star catalogue with linear corrections for Bordeaux measurements of $\Delta\delta$ (solution A5, DATA IIb) the best osculating orbit given here. Therefore, this osculating orbit was next used in the analysis of dynamical evolution of C/1890 F1 presented in section 6. Additionally, the (O-C)-distribution is Gaussian only in this case.

Fig. 3 shows the gap in observations toward the end of data set that stretches from 1891 May 29 to 1892 Jan 7 (seven months). After that gap, the comet was observed only by S. Javelle from Nice Observatory who took nine positional

Table 5. Osculating orbits of C/1890 F1 Brooks determined by Strömgren (1896) and by the present investigation. Our orbital elements of osculating heliocentric orbits are given for three alternative sets of data and two methods of further data processing. The successive columns present: [1] – Epoch of osculation, type of solution (A1: unweighted data, A5: weighted data), and quality of orbit (1a or 1b) estimated using modified method of quality assessment (Królikowska & Dybczyński 2013), [2] – perihelion time [TT], [3] – perihelion distance, [4] – eccentricity, [5] – argument of perihelion (in degrees), equinox J2000.0, [6] – longitude of the ascending node (in degrees), equinox J2000.0, [7] – inclination (in degrees), equinox J2000.0, [8] – reciprocal semi-major axis in units of 10^{-6} AU^{-1}, and [9] – rms and number of residuals used for orbit determination. Osculating orbits determined for weighting data are indicated by light grey shading.

Epoch [yyyymmdd] Type of solution, Quality of orbit [1]	T_{obs} [yyyymmdd.dddddd] [2]	q_{obs} [AU] [3]	e_{obs} [4]	ω_{obs} [°] [5]	Ω_{obs} [°] [6]	i_{obs} [°] [7]	$1/a_{obs}$ [10^{-6}AU^{-1}] [8]	rms, Number of residuals [9]
Osculating orbit determined by Elis Strömgren (original Rayet corrections for Bordeaux measurements of $\Delta\delta$ are included)								
18900317	18900602.033026	1.90758325	1.00041030	68.934397	320.345283	120.556094	Strömgren (1896)	
class: 1A	±0.000447	±0.00000307	±0.00001300	±0.000231	±0.000096	±0.000064	equator & equinox: 1890	
18900602	18900602.037500	1.90758200	1.00026600	68.927300	321.877900	120.569000	MWC08	
Present investigation on the basis of 888 measurements and PPM star catalogue								
Type of data: DATA_Ia								
18900602	18900602.037418	1.90757866	1.00030730	68.927555	321.877730	120.568830	−161.09	2.″94
A5, class: 1a	±0.000294	±0.00000217	±0.00000763	±0.000145	±0.000043	±0.000047	± 4.00	1591
Type of data: DATA_Ib (original Rayet corrections for Bordeaux measurements of $\Delta\delta$ are included)								
18900602	18900602.037782	1.90757411	1.00027856	68.927521	321.877534	120.568981	−146.03	4.″30
A1, class: 1b	±0.000471	±0.00000329	±0.00001251	±0.000241	±0.000086	±0.000070	± 6.56	1598
18900602	18900602.037418	1.90757887	1.00030640	68.927548	321.877721	120.568824	**−160.62**	2.″89
A5, class: 1a	±0.000291	±0.00000215	±0.00000758	±0.000143	±0.000043	±0.000047	± **3.97**	1592
Present investigation on the basis of 908 measurements and Tycho-2 star catalogue								
Type of data: DATA_IIa								
18900602	18900602.037518	1.90757958	1.00032677	68.927671	321.877701	120.568916	−171.30	3.″18
A5, class: 1a	±0.000274	±0.00000200	±0.00000699	±0.000133	±0.000039	±0.000043	± 3.66	1681
Type of data: DATA_IIb (linear corrections for Bordeaux measurements of $\Delta\delta$ are included)								
18900602	18900602.038077	1.90757261	1.00029412	68.927720	321.877503	120.569119	−154.18	3.″95
A1, class: 1b	±0.000421	±0.00000292	±0.00001121	±0.000217	±0.000078	±0.000061	± 5.88	1659
18900602	18900602.037682	1.90758152	1.00033162	68.927751	321.877680	120.568896	−173.84	2.″61
A5, class: 1a	±0.000236	±0.00000173	±0.00000658	±0.000116	±0.000037	±0.000037	± 3.45	1644

measurements in the period from January 7 to February 5, as was mentioned in section 2. Those days the comet was more than 6 au from the Sun, and more than 5.5 au from the Earth. He noted that the comet 'was extremely weak, very badly defined, and one minute wide at most' (citation after Cometography, Kronk 2013). In Fig. 3 one can see that these observations are well-distributed around the orbital solution in declination. However all measurements in right ascension give negative residuals regardless whether the orbit was determined using unweighted (upper panel) or weighted data (middle panel, note small weights of this set of observations). On the other hand, these measurements are very important, because they extend the period of observations by more than eight months and thereby determine the good quality of the orbit. Apart from this trend in right ascension at the end of data, no other systematic trends in the remaining residuals are seen in the O-C diagram based on weighted data. As for the modern standards, large scatter of residuals around the orbit based on unweighted data (upper panel of Fig. 3) draws our attention. It was, however, not unusual at that time.

Fig. 4 compares our best osculating orbit (solution A5 based on DATA_IIb, blue point with solid blue error bars in the figure) with the rest of grid of osculating orbits derived here, and with Strömgren solution given in MWC 08, that is recalculated for the same epoch of 1890 June 2 (and standard equator and equinox: 2000.0) as all of our solutions discussed here (see also Table 5). This figure presents six

Figure 4. Projection of the 6D space of 5 001 clones of C/1890 F1 onto six chosen planes of osculating orbital elements for solution A5 obtained using our best version of observations (DATA_IIb. i.e. recalculated using Tycho-2 star catalogue and applying linear corrections for Bordeaux measurements of $\Delta\delta$). Vertical axes given in the right-hand panels are exactly the same as the vertical axes in the left-hand panels. Each grey point represents a single virtual orbit, while the large blue points with solid error bars represent the nominal weighted orbital solution for DATA_IIb given in Table 5. The analogous solution derived using weighted observations in the DATA_Ib-version are given also by blue dots inside the dotted error bars. The remaining solutions given here are shown using red dots (solutions A5: DATA_IIa, DATA_Ia), magenta squares (A1: DATA_IIa, DATA_Ia), cyan squares (A1: DATA_IIb, DATA_Ib), and green triangles which represent the solution obtained by Strömgren. The zero point of each axis is centred on the nominal values of the respective pair of osculating orbital elements denoted by the subscript '0' for the best solution (A5, DATA_IIb; see also Table 5) and error bars show 1σ errors.

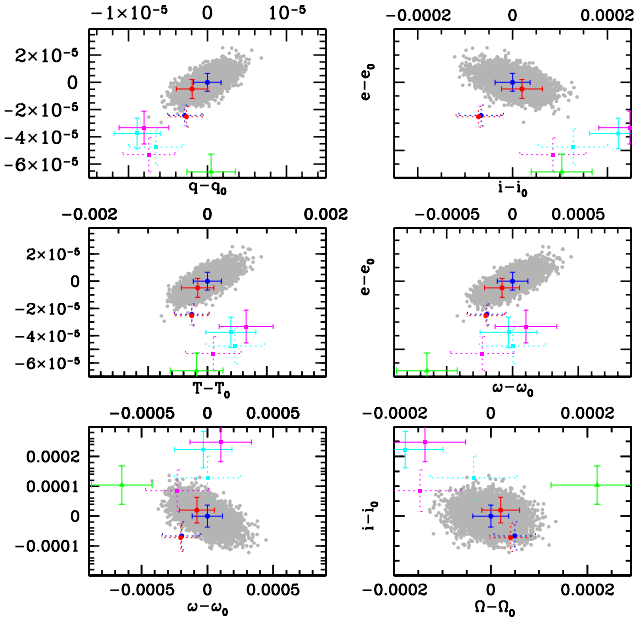

two-dimensional projections which indicate to what extend all these solutions are compatible. From the comparison of all the solutions shown in Fig. 4 and given in Table 5 we can draw following conclusions.

- All osculating orbits, including the solution obtained by Strömgren, are consistent within 3-4σ-combined error, whereas all our weighted solutions are consistent within 1-2σ-combined error (blue and red points).
- The differences in orbital elements between respective pairs of solutions that differ only in ignoring or including the $\Delta\delta$-corrections to Bordeaux measurements, are always deeply below 1σ-combined error for each of the orbital elements (compare respective pairs of blue and red dots, and magenta and cyan dots). The pairs of respective orbits derived using weighted data based on PPM catalogue (blue and red dots with dotted error bars) are closer to each other than pairs of weighted data based on Tycho-2 catalogue (blue and red dots with solid error bars). In order to understand this behaviour we recommend to analyse the weights given in Table 4 for Bordeaux observations and for different versions of data.
- Orbital element uncertainties obtained by Strömgren are very similar to those derived by us using the unweighted data (A1-type of solutions, cyan and magenta error bars).
- Osculating orbits based on weighted data are characterized by significantly smaller orbital element uncertainties than those given by Strömgren. He obtained his solution by using the $\Delta\delta$-correction for Bordeaux measurements, and somehow weighting the data when compressed into 16 normal points. Thus, we conclude that both methods used herein and based on two different modern catalogues give significantly better quality of orbits.
- Using the Tycho-2 catalogue to recalculate all measurements of C/1890 F1, and applying all necessary corrections, we also derived the best quality of osculating orbit (solution A5, DATA_IIb shown in Fig. 4 as a blue dots with solid error bars).
- The method based on automatic search for stars in PPM star catalogue proposed by Gabryszewski (1997) allowed to recalculate 50 per cent of measurements. This also significantly improves the orbit quality and provides a solution (blue point with dotted error bars) within 2σ-combined error from our best one.

Table 6. Original and future barycentric inverse semimajor axes for grid of orbital solutions of C/1890 F1. Values determined using solutions based on weighting data are indicated by light grey shading.

Solution type	$1/a_{\rm ori}$ [in units of au^{-6}]	$1/a_{\rm fut}$	$1/a_{\rm fut} - 1/a_{\rm ori}$
Type of data: DATA_Ia			
A1	79.35 ± 6.84	116.15 ± 6.84	36.796 ± 0.004
A5	67.05 ± 3.96	103.85 ± 3.96	36.798 ± 0.002
Type of data: DATA_Ib			
A1	82.13 ± 6.63	118.93 ± 6.63	36.794 ± 0.004
A5	67.60 ± 3.95	104.40 ± 3.95	36.797 ± 0.002
Type of data: DATA_IIa			
A1	71.77 ± 6.25	108.59 ± 6.24	36.802 ± 0.004
A5	56.91 ± 3.71	93.71 ± 3.71	36.803 ± 0.002
Type of data: DATA_IIb			
A1	74.02 ± 5.85	110.82 ± 5.85	36.800 ± 0.003
A5	54.37 ± 3.42	91.18 ± 3.42	36.805 ± 0.002

5 ORIGINAL AND FUTURE BARYCENTRIC ORBITS

To be able to reliably follow the evolution of cometary orbit we must also know the orbital uncertainty [10] at each

[10] that results from the observational uncertainty of the osculating orbit, see Table 5

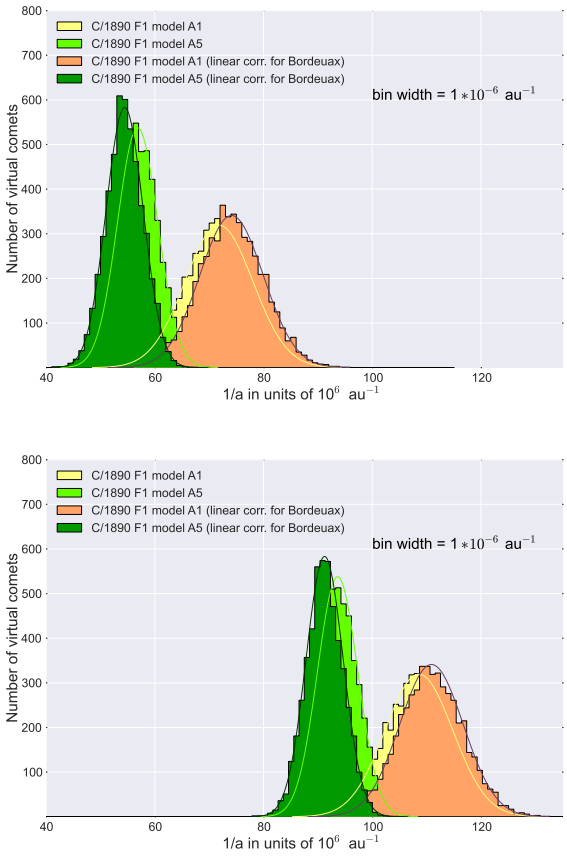
C/1890 F1 model A1
C/1890 F1 model A5
C/1890 F1 model A1 (linear corr. for Bordeuax)
C/1890 F1 model A5 (linear corr. for Bordeuax)
bin width = 1 ∗10^−6 au^−1
Number of virtual comets
1/a in units of 10^6 au^−1

Figure 5. Original (upper panel) and future (lower panel) $1/a$-distributions for solutions based on data recalculated with the use of the Tycho-2-catalogue. Each histogram represents the distribution of 5001 virtual comets (VCs), where the Gaussian function (continuous line) gives perfect fit in each case. The vertical axis shows counts in each bin within the sample of 5001 clones considered in each case; it means that counts of 500 VCs gives a probability of 0.1.

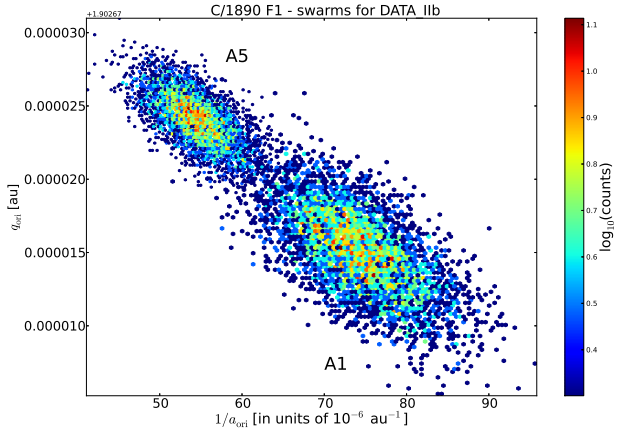

Figure 6. Projection of two original swarms of 5001 VCs (6D each) of C/1890 F1 Brooks onto the $1/a$–q plane. These swarms represent solutions derived from DATA_IIb type of data, where the less dispersed swarm (upper left, and given by dark-green histogram in Fig. 5) represents the A5-solution based on data which were weighted during the procedure of orbit determination, whereas the more disperse swarm shows A1-solution (given by sandy-brown histogram in the upper-left panel of Fig. 5). Density distribution of A5-swarm is superimposed on the more dispersed A1-swarm. Density map is given in logarithmic scale which is presented in the individual panel given on the right. Note that the value of the beginning of vertical axis is given just above the upper horizontal border of the plot.

moment of our numerical calculations. Therefore for each solution given in Table 5 a swarm of 5001 VCs, including the nominal orbit, was constructed according to a Monte Carlo method given by Sitarski (1998), for more details see also Królikowska et al. (2009). Next, the dynamical calculations of each swarm of VCs were performed backwards and forwards in time until each VC reached 250 au from the Sun, that is, a distance where planetary perturbations are completely negligible. This method allowed us to determine the uncertainties of original and future orbital elements by fitting any orbital element distribution in the swarm to Gaussian distribution at each moment of dynamical evolution.

All the original and future barycentric $1/a$-values are given in Table 6 whereas the full original and future orbits are presented at `http://ssdp.cbk.waw.pl/LPCS` and `http://apollo.astro.amu.edu.pl/WCP`. The distributions of these original and future swarms of $1/a$ are shown in Fig. 5, where the Gaussian fits to these distributions are also plotted. We conclude that the best solution (DATA_IIb, version A5) gives the values of 54.37±3.42 and 91.18±3.42, in units of 10^{-6} au^{-1}, for original and future $1/a$, respectively. Both are the smallest values among all respective solutions given in Table 6. Strömgren (1914) gives a value of 71.8 in the same units for original $1/a$, and this value was cited by Sinding (1948), and next it was taken by Oort for his famous analysis of $1/a_{\rm ori}$-distribution.

The mutual proximity of swarms A1 and A5 obtained using Tycho-2 (DATA_IIb) in two-dimensional projection is visualized in Fig. 6. Similar overlapping of the swarms we can find in every other projection.

It is worth noting that C/1890 F1 is very interesting from the planetary perturbations point of view: it suffered very small perturbations from planets during its passage through a planetary zone in the observed 1890-1892 apparition. Regardless of the version of data used, these perturbations are at the level of $\delta(1/a) = 1/a_{\rm fut} - 1/a_{\rm ori} \simeq 36.8 \times 10^{-6}$ au^{-1} (last column of Table 6). As a result, according to the best solution, the comet will be still inside the Oort spike in the next apparition.

Table 7 gives other examples of comets that were subjected to weak planetary perturbations. All were selected from the sample of about 160 Oort spike comets investigated by us so far. Here, we only present comets with small perihelion distance of $q_{\rm obs} < 3.5$ au, just as we have in the case of comet C/1890 F1. However, we have also recognized another 25 objects of that kind with large $q_{\rm obs}$ which constitute a significant percentage of these large perihelion objects (for more details see discussion in Dybczyński & Królikowska (2011)). Otherwise, thirteen comets presented here (twelve from Table 7 plus C/1890 F1) make up only about 15 per cent of small perihelion Oort spike comets. Among them five objects have orbits almost perpendicular to the ecliptic

plane and move on retrograde orbits, these are shown using light grey shading in Table 7. When we further reduce the sample to comets that have passed to more bound orbit during the passage through planetary zone we find only six such cases. Therefore, we can say that because of suffering such a small planetary perturbations the dynamical behaviour of C/1890 F1 is unusual among small perihelion comets.

6 PREVIOUS AND NEXT PERIHELION PASSAGES

With original and future barycentric orbits at hand, we can study past and future motion of C/1890 F1 Brooks by following its motion numerically. At distances greater than 250 au we ignore all planetary perturbations but we include Galactic and stellar perturbations and integrate the comet motion to the previous and next perihelion passage, that is about 2.5 Myr to the past and 1.1 Myr to the future. Since previous and next perihelion passages of C/1890 F1 are deep in the planetary zone and we cannot calculate planetary perturbations at these epochs, we have to stop our calculations at these moments. Of course for that reason one should treat our previous orbit as the osculating one when the comet left the planetary zone after the previous perihelion. Analogously one should treat the next orbit as the osculating one before the comet will enter the planetary zone during its next apparition.

In this investigation we used exactly the same dynamical model as in Paper 5. It includes Galactic disc and Galactic Centre tidal terms and perturbations from 90 stars or stellar systems known to pass closer than 3.5 pc from the Sun in the past, currently or in the future. Since we study C/1890 F1 motion in an interval smaller than 4 Myrs these stellar data can be considered complete in terms of massive and slow moving perturbers, see Paper 5 for the detailed discussion and the description of the stellar perturbers list. Stellar perturbers, together with a comet, are numerically integrated as the N-body problem in the Solar system barycentric frame with additional Galactic tidal potential. This calculation has been repeated for the nominal orbit of this comet and for all 5000 VCs to propagate observational uncertainties.

Past and future motion of C/1890 F1 is quite regular, all previous and next orbital clones move on elliptical orbits in each of the analysed swarms. The most important parameters of these orbits are given in Table 8. We present here the results of two different calculations - with and without stellar perturbations - in order to show how small their influence is. In contrast to almost perfectly normal distributions of the inverse semimajor axes in all of the analysed solutions, the perihelion and aphelion distances have non-Gaussian distributions (see also Fig. 8). Therefore, in Table 8 we describe the distribution of $q_{\rm prev}$, $q_{\rm next}$, $Q_{\rm prev}$ and $Q_{\rm next}$ by presenting their median values accompanied with 10th and 90th deciles.

As it was highlighted in Section 5 comet C/1890 F1 Brooks suffered only small planetary perturbations during its observed perihelion passage. Looking in a wider perspective we see that it was observed in a decreasing phase of its perihelion distance evolution due to the Galactic tides. The

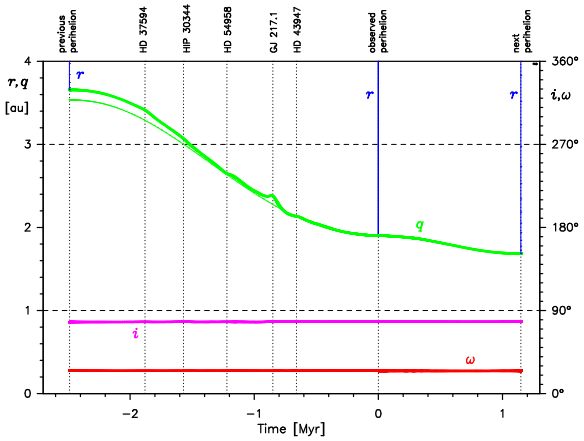

Figure 7. Past and future evolution of C/1890 F1 nominal orbit of the preferred solution under the simultaneous Galactic and stellar perturbations.

perihelion distance decreases from $q_{\rm prev} = 3.64$ au through $q_{\rm obs} = 1.91$ au down to $q_{\rm next} = 1.69$ au. Taking into account only small semimajor axis shortening by planetary perturbations, C/1890 F1 is an example of the Oort spike comet visiting deep interior of the Solar system (and therefore being observable) in at least three consecutive perihelion passages, still being a member of the spike. This behaviour is clearly shown in Fig. 7.

Many interesting aspects of the past and future orbit evolution of C/1890 F1 under stellar and Galactic perturbations can be found in Fig.7. In this picture the horizontal time axis extends from the previous perihelion passage through the observed apparition up to the next perihelion passage. The left vertical axis is expressed in au and describes the osculating perihelion distance evolution (q, green line), as well as the heliocentric distance plot (r, thin blue lines). Due to the time scale of this picture, the heliocentric distance plots take a form of vertical blue lines exactly at perihelion passage moments. The right vertical axis is expressed in degrees and describes changes in the osculating inclination (i, magenta line) and in the argument of perihelion (ω, red line). Both of these angular elements are expressed in the Galactic frame. All thick lines depict dynamical evolution under joint stellar and Galactic perturbations, while the thin lines mark the evolution with the stellar perturbations excluded. Horizontal dashed lines draw attention to the beginning of the second and fourth quarter of ω, whose values (90°and 270°) are important from the point of view of the Galactic perturbations (crossing these lines coincides with perihelion distance minimum). The vertical dashed lines show the closest approaches of a comet with the star or stellar system, which name is placed at the top of the picture. It is worth mentioning that the timing of the stellar perturbation is not necessarily strictly aligned with this closest approach moment – it strongly depends on the geometry, since the final heliocentric orbit change is a net effect of a stellar gravitational action on both a comet and the Sun. The action of GJ 217.1 is a good example of a frequent self-cancelling stellar action: the perturbation gained during the approaching phase is then cancelled during the receding

Table 7. Original and future barycentric inverse semimajor axes and their $\Delta 1/a = 1/a_{\rm fut} - 1/a_{\rm ori}$ differences for other Oort spike comets subjected to a weak planetary perturbations during observed perihelion passage through the planetary zone ($|\Delta 1/a| < 100$ in units of 10^{-6}au^{-1}). Comets with perihelion distance closer than 3.5 au to the Sun are only presented here. Original and future $1/a$-values were taken from Królikowska (2014) and Królikowska et al. (2014). Comets with inclination to ecliptic inside the range of 80°– 100°(all on retrograde orbits, see column [7]) are indicated by light grey shading.

Comet	$1/a_{\rm ori}$	$1/a_{\rm fut}$	$\Delta(1/a)$	1σ-error	quality	$q_{\rm obs}$	$i_{\rm obs}$
	in units of 10^{-6}au^{-1}				class	[au]	degrees
[1]	[2]	[3]	[4]		[5]	[6]	[7]
C/1913 Y1 Delavan	52.57 ± 4.23	86.84 ± 4.23	+34.27	< 0.01	1a	1.1	68.2
C/1919 Q2 Metcalf	34.7 ± 67.3	-26.9 ± 67.3	−61.56	0.05	2a	1.1	46.4
C/1946 P1 Jones	50.86 ± 5.08	22.55 ± 5.08	−28.32	< 0.01	1a	1.1	57.0
C/1946 U1 Bester	17.08 ± 6.52	43.88 ± 6.52	+26.80	< 0.01	1b	2.4	108.2
C/1947 Y1 Mrkos	28.89 ± 8.49	54.31 ± 8.50	+25.42	< 0.01	1b	1.5	77.5
C/1948 E1 Pajdušáková-Mrkos	37.25 ± 2.74	35.21 ± 2.74	−2.04	< 0.01	1a	2.1	92.9
C/1952 W1 Mrkos	-0.1 ± 85.8	-41.4 ± 106.9	−40.6	43.3	2a	0.8	97.2
C/1989 Q1 Okazaki-Levy-Rudenko	42.9 ± 22.2	80.5 ± 27.3	+37.6	46.6	2a	0.6	90.1
C/1997 J2 Meunier-Dupouy	44.64 ± 0.88	14.72 ± 0.91	−29.92	1.47	1a+	3.1	91.3
C/2006 HW_{51} Siding Spring	47.31 ± 3.37	90.12 ± 3.37	+42.81	< 0.01	1a	2.3	45.8
C/2006 S2 LINEAR	72.52 ± 8.14	-10.77 ± 18.09	−83.3	25.5	1b	3.2	99.0
C/2007 Q3 Siding Spring	39.13 ± 0.49	118.96 ± 0.96	+79.83	< 0.01	1a+	2.3	65.7

Table 8. C/1890 F1 previous and next orbital parameters derived from DATA_IIb set of observation. The inverse semimajor axis is presented as the Gaussian mean value and its 1σ uncertainty; $T_{\rm prev}$ and $T_{\rm next}$ are epochs of the previous and next perihelion respectively. Perihelion and aphelion distances, as well as their epochs are presented as 10th : 50th (the median) : 90th-deciles due to departure of their distributions from a normal one. Solution name subscripted with a star means that all known stellar and Galactic perturbations were included in the numerical integrations, in contrast to the solutions without subscripts, where only Galactic perturbations were included.

Solution	$T_{\rm prev}$ [Myr]	$1/a_{\rm prev}$ [10^{-6}au^{-1}]	$q_{\rm prev}$ [au]	$Q_{\rm prev}$ [10^3au]	$T_{\rm next}$ [Myr]	$1/a_{\rm next}$ [10^{-6}au^{-1}]	$q_{\rm next}$ [au]	$Q_{\rm next}$ [10^3au]
$A5_*$	−2.81:−2.48:−2.20	$+54.44 \pm 3.42$	3.17:3.64:4.35	34.0:36.8:40.0	1.07:1.15:1.24	$+91.24 \pm 3.42$	1.65:1.69: 1.72	20.9:21.9:23.0
A5	−2.81:−2.48:−2.20	$+54.44 \pm 3.42$	3.09:3.53:4.20	34.0:36.8:40.0	1.07:1.15:1.24	$+91.24 \pm 3.42$	1.65:1.69: 1.72	20.9:21.9:23.0
$A1_*$	−1.83:−1.56:−1.35	$+74.17 \pm 5.85$	2.27:2.42:2.67	24.5:27.0:30.0	0.78:0.86:0.96	$+110.91 \pm 5.85$	1.76:1.79: 1.81	16.9:18.0:19.3
A1	−1.83:−1.56:−1.35	$+74.12 \pm 5.85$	2.25:2.40:2.64	24.5:27.0:30.0	0.78:0.86:0.96	$+110.92 \pm 5.85$	1.76:1.79: 1.82	16.9:18.0:19.3

phase. During the presented 3.5 Myr interval of cometary evolution, the Galactic and stellar perturbations are notable only in the perihelion distance, while being infinitesimally small in angular elements. We have not identified any profound stellar perturbation in future motion of C/1890 F1 since it will depart from the Sun for only about 20 000 au and it will complete its future orbital revolution (1.1 Myr) about 0.3 Myr before the predicted close flyby of the star Gliese 710. Other stars are too small and/or too distant to noticeably change the future orbit of this comet.

C/1890 F1 is definitely the dynamically old comet. Even the most protruding clones in our swarm of VCs have the previous perihelion distance well below 10 au. The osculating perihelion distance and the inverse semimajor axis distributions of C/1890 F1 for the moment of the previous perihelion passage (nominally 2.5 Myr ago) are presented in Fig. 8. It is worth mentioning that the presented $1/a$-distribution is still almost perfectly Gaussian while the q-distribution significantly departs from the normal one, mainly as a result of Galactic perturbations. The central, black joined distribution corresponds to the smaller cloud of 5001 VCs presented in Fig. 6 after the 1.7–3.8 Myr of backward dynamical evolution under the simultaneous Galactic and stellar action (different VCs have different orbital periods, a nominal value equals 2.5 Myr, the fastest VC was at the previous perihelion 1.7 Myr ago while the slowest one almost 3.8 Myr ago).

The time-spread (along horizontal axis) and the space-spread (along vertical axis) of our swarms of VCs in previous and next perihelion are clearly visualized in Fig. 9.

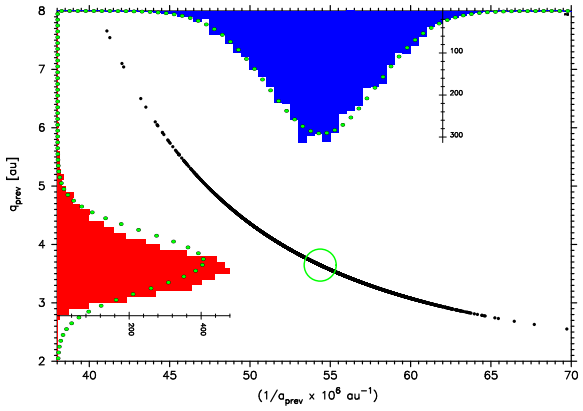

Figure 8. Joint and marginal distributions of the osculating $1/a$ and q of 5001 VCs derived from the nominal orbit of the preferred solution for C/1890 F1, stopped at their previous perihelion passage. The centre of the green circle marks the nominal values. Small green dots overprinted on the marginal distributions show best-fitting Gaussian distributions.

We presented here changes in the barycentric distance of all 5001 VCs from two different solutions of orbit determination, both based on the DATA_IIb set of observations. The red (darker) swarm depicts the distribution evolving from the osculating orbit fitted to the weighted observations (A5-solution) while the green (grey) one depicts the evolution of swarm constructed without weighting (A1-solution). Nominal orbits for both of our solutions are marked as black

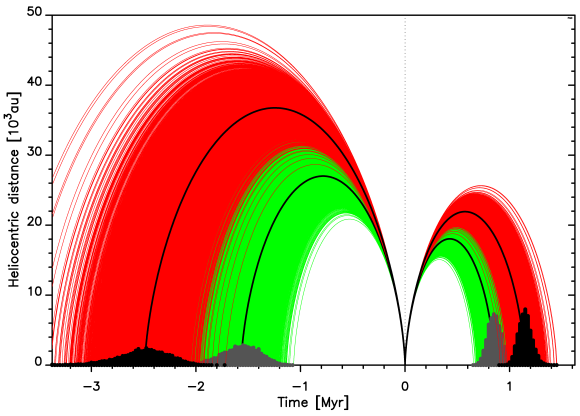

Figure 9. Past and future swarms of C/1890 F1 orbits for two different solutions based on the DATA_IIb set of observations: red (dark grey) lines represent results for A5 solution (preferred, weighted data) while green (light grey) lines correspond to the A1 solution (without data weighting, see Tables 6 and 8 for more details). All known stellar and Galactic perturbations were taken into account. Black lines depict nominal orbits evolution. Distributions of previous and next perihelia epochs are also shown.

curves. Thus, this figure shows also how the data handling can change the results during the evolution to the previous/next perihelion distance (see also Table 8). The dynamical evolution of Strömgren's orbit would be very similar to the evolution of our A1 orbital solution. We conclude that our preferred A5-solution gives longer previous and next orbital periods of about 2.5 and 1.1 Myr respectively. As a result, Galactic perturbations act more effective during the evolution, and for this solution we get a greater change of the perihelion distances between three consecutive perihelion passages analysed here.

7 SUMMARY AND CONCLUSIONS

A rich observational material of C/1890 F1 Brooks allows to test whether it is productive to recalculate with the use of modern star catalogues the original positions of comets discovered long ago. During this study we compared two distinct algorithms:

- automatic search for reference stars in the PPM star catalogue according to Gabryszewski (1997), which was frequently used by us when we only have ($\mathscr{O}$−⋆)-measurements and data on the positions of comets,
- automatic search for reference stars in the Tycho-2 star catalogue on the basis of mean coordinates of reference stars used by all observers, and next, a detailed analysis of all the cases of large residuals in the observed comet's positions, resulting from the star search (∼30 per cent of all observations in the case of C/1890 F1).

The first method was successfully used several times before, and more recently by Królikowska et al. (2014). This method of automatic search for stars in PPM catalogue recalculates about 50 per cent of the existing data of C/1890 F1. The second method was developed for the present investigation. In the SIMBAD database we have successfully found all stars used by observers more than hundred years ago to calculate the comet's position in α and/or δ from ($\mathscr{O}$−⋆)-measurements. It means, that all positions of C/1890 F1 were recalculated here using these original ($\mathscr{O}$−⋆)-measurements ($\Delta\alpha$ and/or $\Delta\delta$). We decided to use stellar positions and proper motions from the Tycho-2 catalogue for that purpose.

It should be emphasized that thanks to the monumental publication by Elis Strömgren (1896), our task has become much easier, though, it was still time consuming. Searching for stars in the SIMBAD database would be more difficult without the mentioned publication, particularly in the more complicated cases. In addition, thanks to Strömgren's deep analysis of data, it turned out that one should take into account corrections to $\Delta\delta$ measurements from Bordeaux Observatory (we prefer linear version of these corrections as described in section 3.2). However, these corrections change the orbital solution on the significantly lower level than the use of modern stellar data. For example, a solution based on data recalculated in about 50 per cent (PPM catalogue, DATA_Ia/DATA_Ib) differs a lot from the respective solution based on fully recalculated data (Tycho-2 catalogue DATA_IIa/DATA_IIb) than any two solutions based on data with and without Bordeaux corrections. Moreover, the Bordeaux corrections are also much less important than the method of data treatment. This is clearly shown in Fig. 5, where we can see that light-green histogram (weighted data, corrections for Bordeaux omitted) is very similar to dark-green histogram (weighted data, corrections for Bordeaux applied), however, it differs significantly from the pair of yellow/orange histograms based on unweighted data.

Next, we have shown that both search algorithms for contemporary data for the reference stars resulted in a significant reduction of the uncertainties of orbital elements in the case of C/1890 F1 Brooks. The comparison of our solutions with that derived by Strömgren is presented in Table 5 and Fig. 4. By analysing all these models, we concluded that the orbital solution based on DATA_IIb (all positional observations were recalculated using Tycho-2 catalogue and next weighted) gives the most reliable, and also the most accurate osculating orbit.

Using this most preferred orbital solution (and its unweighted variant for comparison, see Fig. 9) we numerically followed a motion of C/1890 F1 for one orbital period to the past and to the future. Starting from full swarms of original and future VCs orbits we obtained previous and next orbital elements of this comet together with their uncertainties. All known stellar and Galactic perturbations were fully taken into account but for comparison purposes we have also performed the calculations in which stellar perturbations were ignored. This comparison (see Table 8 for details) shows that none of known stellar perturbers significantly change the past and future motion of C/1890 F1 during the three successive perihelion passages analysed here. It should be stressed that due to relatively short past orbital period of C/1890 F1 Brooks (nominally 2.5 Myr) it seems rather improbable that we have missed here some unknown but significant (i.e. massive and/or slow moving) and nearby stellar perturber.

Three consecutive perihelion passages of this comet (the time interval of about 3.6 Myr) clearly indicate that this comet deeply penetrates the planetary region during each of them (below 5 au from the Sun, see Table 8) and easily crosses the so-called Jupiter-Saturn barrier. Therefore,

we conclude that C/1890 F1 Brooks is a dynamically old comet and additionally, as a result of negligible planetary perturbations during the observed apparition, it will remain a member of the Oort spike during the next apparition. Note that Oort (1950) treated this comet (by definition) as a dynamically new one and used it in support for his cometary cloud hypothesis.

Currently, on the basis of analysis of 109 Oort spike comets, we estimate that about 50 per cent of them are dynamically old. However, the percentage of dynamically old comets grows up to almost 90 for comets with $1/a_{\rm ori}$ inside the range of 0.000040–0.000100 $\rm au^{-1}$ (Dybczyński & Królikowska 2015). Thus, the past dynamical evolution of comet Brooks having $1/a_{\rm ori}$ greater than 0.000050 $\rm au^{-1}$ is not surprising. On the other hand, for the reason of very weak planetary perturbations one can say that the dynamical behaviour of C/1890 F1 is unusual among small perihelion comets.

In the near future, we plan to deal with all near-parabolic comets discussed by Oort (1950) as well as all Oort spike comets discovered in the years 1901–1950 to answer the question about their source from the previous perihelion perspective, and make our sample of near-parabolic comets with known previous and next orbital elements more complete. It can also happen that some comets observed on a more tightly bound orbit ($1/a_{\rm obs} > 0.000100\,\rm au^{-1}$) will contribute to a future $1/a$-distribution as Oort spike comets. Therefore the extension of our research to objects with $1/a$ similar to that shared by C/2013 V2 Borisov ($1/a_{\rm ori} = 0.000770\,\rm au^{-1}$and $1/a_{\rm fut} = 0.000089\,\rm au^{-1}$, Nakano (2015)) seems to be important to put our investigation in the broader framework of dynamical evolution of long-period comets.

Some auxiliary material to this paper is available at `http://ssdp.cbk.waw.pl/LPCS` and `http://apollo.astro.amu.edu.pl/WCP`.

8 ACKNOWLEDGEMENTS

We are very grateful to Ryszard Gabryszewski for providing software and related assistance with the search for stars in PPM star catalogue. We also thank the anonymous referee of this paper for valuable remarks. This research has made use of NASA's Astrophysics Data System Bibliographic Services and of the the SIMBAD database and VizieR catalogue access tool, CDS, Strasbourg, France, and was partially supported from the project 2015/17/B/ST9/01790 founded by National Science Centre in Poland.

REFERENCES

Brooks W. R., 1890, MNRAS, 50, 375
Dybczyński P. A., 2001, A&A, 375, 643
Dybczyński P. A., Królikowska M., 2011, MNRAS, 416, 51
Dybczyński P. A., Królikowska M., 2015, MNRAS, 448, 588
Fernández J. A., ed. 2005, Comets - Nature, Dynamics, Origin and their Cosmological Relevance Astrophysics and Space Science Library Vol. 328
Gabryszewski R., 1997, Planetary and Space Science, 45, 1653
Høg E., et al., 2000, A&A, 355,
Kronk G. W., 2003, Cometography. A Catalog of Comets. Volume 2. 1800–1899
Królikowska M., 2014, A&A, 567, A126
Królikowska M., Dybczyński P. A., 2010, MNRAS, 404, 1886
Królikowska M., Dybczyński P. A., 2013, MNRAS, 435, 440
Królikowska M., Sitarski G., Sołtan A. M., 2009, MNRAS, 399, 1964
Królikowska M., Sitarski G., Pittich E. M., Szutowicz S., Ziołkowski K., Rickman H., Gabryszewski R., Rickman B., 2014, A&A, 571, A63
Marsden B. G., Williams G. V., 2008, Catalogue of Cometary Orbits 17th Edition. Smithsonian Astrophysical Observatory, Cambridge, Mass.
Marsden B. G., Sekanina Z., Everhart E., 1978, AJ, 83, 64
Nakano S., 2015, Nakano Note 2952, URL http://www.oaa.gr.jp/ oaacs/nk/nk2952.htm
Oort J. H., 1950, Bull.Astron.Inst.Nether., 11, 91
Perryman M. A. C., et al., 1997, A&A, 323,
Roeser S., Bastian U., 1988, Astronomy and Astrophysics Supplement Series, 74, 449
Sinding E., 1948, Pub. Copenhagen Obs., 146
Sitarski G., 1998, Acta Astronomica, 48, 547
Strömgren E., 1896, Berechnung der Bahn des Kometen 1890II
Strömgren E., 1914, Publ. Obs. Copenhagen, 19, 189
Superintendent of the US Naval Observatory (probably Phythian, R.L.), 1890, AJ, 10, 63
Yabushita S., 1989, AJ, 97, 262
Zacharias N., Finch C. T., Girard T. M., Henden A., Bartlett J. L., Monet D. G., Zacharias M. I., 2013, AJ, 145, 44

This paper has been typeset from a TEX/LATEX file prepared by the author.